J Geophys (1987) 61:158–167

Journal of Geophysics

Surface harmonic expansion methodology in restricted domains of the Earth's surface – Application to the Indian Ocean

Xavier Lana and Ramon Carbonell

Departamento de Geodinamica, Geofisica y Paleontologia, Facultad de Fisica, Avenida Diagonal 645, E-08028 Barcelona, Spain

Abstract. A dense distribution of Rayleigh-wave group velocities (fundamental mode) throughout the Indian Ocean is obtained by means of spherical harmonic expansion of the inverse of group velocity and standard least-squares methods. The data, covering the whole region, come from nine earthquakes in the Indian Ocean, recorded at several stations of the WWSSN (long period). This coverage, for each period, consists of approximately 50 paths. The records used correspond to periods ranging between 15 and 90 s. The results allow a qualitative discussion of the upper part of the Indian Ocean's lithosphere and especially display high velocities around the Rodrigues triple junction. The number of group velocities mapped should allow a quantitative study of the upper part of this lithosphere.

Key words: Spherical harmonic expansions – Group velocities of Rayleigh waves' fundamental mode – Indian Ocean – Lithosphere

Introduction

The spherical harmonic expansion method is an efficient tool in work on many aspects of Earth properties on a global scale. Some pioneer works are the papers of Kaula (1959), Horai and Simmons (1969), Ellsasser (1966) and Coode (1967), among others. These papers developed both atmospheric and geophysical parameters for the whole Earth. Dispersive properties of surface waves have also been subjected to this analysis by Sato and Santo (1969). More recent papers which follow the same line are by Nakanishi and Anderson (1982), Nataf et al. (1984), Nishimura and Forsyth (1985) and others. Nishimura and Forsyth's (1985) study is the only one which develops surface-wave properties by means of a spherical harmonic representation on a restricted domain of the Earth. Additional information about propagation of body waves and inversion of seismic waveforms, using spherical harmonics, can be found in papers of Dziewonski (1984) and Woodhouse and Dziewonski (1984).

It must be remembered that spherical harmonic expansions have two shortcomings. First, they are no longer efficient when there are very sharp lateral velocity gradients. This problem could be avoided by increasing the harmonic order. Second, if expansions are applied to restricted domains, the properties under investigation near the boundary regions must be carefully considered. The parameters studied in this paper extend over a considerable part of the Earth's surface and, consequently, spherical harmonic functions are a reasonable expansion basis. The linearity between data (travel times) and parameters (spherical harmonic coefficients) must be pointed out, because it simplifies the least-squares method by avoiding iterative processes. Although the pure-path method has the same advantage of linearity, spherical harmonic expansions are superior since they avoid the a priori age regionalization which is an important shortcoming in the first method.

In the present paper we study the methodology involved in the expansion of Rayleigh-wave group velocities by means of spherical harmonics over restricted domains. The implications of this method for crustal and lithospheric structure are outlined.

Theory

Following Courant and Hilbert (1962), any function $g(\theta, \varphi)$ which is continuous, together with its derivatives, up to second order on the sphere may be expanded in an absolutely and uniformly convergent series in terms of spherical harmonics:

$$g(\theta, \varphi) = \sum_{n=0, m=-n}^{\infty, n} G_{nm} \, Y_{nm}^{(\theta, \varphi)}, \tag{1}$$

where θ and φ are the spherical coordinates colatitude and longitude, respectively, $Y_{nm}^{(\theta,\varphi)}$ the fully normalized spherical harmonics and G_{nm} the coefficients of the expansion.

From now on, as we will study the group velocity of the Rayleigh-wave fundamental mode, the function $g(\theta, \varphi)$ will be the corresponding slowness $s(\omega, \theta, \varphi)$; ω is the angular frequency.

We define the travel time for each path l between an epicentre (e) and a station (s) as:

$$t_l = L_l \, S^*(\omega)_l, \tag{2}$$

where L_l is the epicentral distance and $S^*(\omega)_l$ the experimental averaged slowness. The slowness in Eq. (2), in the ap-

Offprint requests to: X. Lana

proximation of geometrical optics, is an average value along the path. Consequently, we can also define the travel time as:

$$t_l=\int_e^s S(\omega, \theta, \varphi)\, dL_l, \tag{3}$$

where $S(\omega, \theta, \varphi)$ is the local slowness and depends on the spherical coordinates.

The pure-path method (Nishimura and Fortsyth 1985; Yu and Mitchell 1979; Mitchell and Yu 1980; and others) assumes a correlation between surface tectonics and deep structure. Under this hypothesis, the product in (2) or the integral in (3) is replaced by a discrete summation for all the structural ages considered. In order to avoid this a priori age regionalization of crustal structure, inherent to the pure-path method, a continuous representation of the slowness on colatitude and longitude is more advisable.

Splitting the fully normalized spherical harmonics into sine and cosine terms, Eq. (1) for $S(\omega, \theta, \varphi)$ reads:

$$S(\omega, \theta, \varphi)=\sum_{n=0,m=0}^{\infty,n} A_{nm}\, P_{nm}^{(\theta)} \cos(m\varphi) + \sum_{n=1,m=1}^{\infty,n} B_{nm}\, P_{nm}^{(\theta)} \sin(m\varphi). \tag{4}$$

$P_{nm}^{(\theta)}$ are the fully normalized associated Legendre functions. It is implicitly assumed that azimuthal anisotropy can be neglected.

Inserting Eq. (4) in Eq. (3), we obtain for each path l ($l=1, \ldots, k$) the basic equation:

$$t_l=\int_e^s \left\{ \sum_{n=0,m=0}^{\infty,n} A_{nm}\, P_{nm}^{(\theta)} \cos(m\varphi) + \sum_{n=1,m=1}^{\infty,n} B_{nm}\, P_{nm}^{(\theta)} \sin(m\varphi)\right\} dL_l. \tag{5}$$

The integrals:

$$C_{nml}=\int_e^s P_{nm}^{(\theta)} \cos(m\varphi)\, dL_l \tag{6a}$$

$$D_{nml}=\int_e^s P_{nm}^{(\theta)} \sin(m\varphi)\, dL_l, \tag{6b}$$

which depend on the location of the epicentre and the station, must be evaluated along the path.

The set of equations, Eq. (5), for different paths can be written in a compact way as follows:

$$\boldsymbol{T}=\boldsymbol{M}\,\boldsymbol{A}, \tag{7}$$

where $\boldsymbol{T}$ is the travel-time vector $(t_1, \ldots, t_k)$, $\mathbf{M}$ is the matrix formed by the factors C_{nml} and D_{nml} defined in Eq. (6) for each path l, and $\boldsymbol{A}$ is the vector of the unknown coefficients A_{nm} and B_{nm} of the spherical harmonic expansion. Expression (7) is a linear system of equations which is solved by means of the standard least-squares method.

Another very important question is the uncertainty of the spherical harmonic coefficients in terms of the errors in the data. Following Nishimura and Forsyth (1985), we can define the slowness variance as:

$$\sigma^2_{S(\theta,\varphi)}=\boldsymbol{Q}\boldsymbol{W}\boldsymbol{Q}^T, \tag{8}$$

where $\boldsymbol{W}$ is the covariance matrix of the coefficients and $\boldsymbol{Q}$ the partial derivative vector, defined as:

$$\boldsymbol{Q}=(\partial S/\partial A_{nm}, \quad \partial S/\partial B_{nm}). \tag{9}$$

The covariance matrix of the coefficients is defined as:

$$\boldsymbol{W}=\boldsymbol{M}^{-1}\,\boldsymbol{\Psi}(\boldsymbol{M}^{-1})^T \tag{10}$$

where $\boldsymbol{M}^{-1}$ is the generalized inverse of $\boldsymbol{M}$ and $\boldsymbol{\Psi}$ the covariance matrix of the data. The covariance of the data is estimated from the travel-time residual of the least-squares process by assuming, for instance, that $\boldsymbol{\Psi}$ is the identity matrix multiplied by the Euclidian norm of the travel-time residual.

If we are interested in the group-velocity variance, it is easy to find that

$$\sigma_{v(\theta,\varphi)}=\sigma_{S(\theta,\varphi)}\, S^{-2}(\theta, \varphi). \tag{11}$$

Methodology

A first and important point is to fix the degree of the spherical harmonic expansion; in other words, to decide how many of the fully normalized harmonics should be used in this expansion. The path coverage of the studied domain, the travel-time residual evolution with the degree of the expansion and the physical relevance of the coefficients will give some insight to this question:

A) It is clear that the path coverage has a direct influence on the degree of the expansion (Nishimura and Forsyth, 1985), but this effect has not been quantified yet.

B) The minimization of the inversion travel-time residuals, as a criterion to decide the convenient degree of the expansion, has been proposed by Nakanishi and Anderson (1982). It consists of choosing the degree that corresponds to a minimum of the travel-time residual evolution. The same authors point out that this criterion will not always work.

C) A low-degree expansion corresponds to a simple view of the Earth model. A higher-degree expansion produces corrections to this poorly detailed description in order to obtain a more realistic model. In this way, when the degree increases, a decrease of the absolute values of the expansion coefficients is expected, provided that only smooth lateral heterogeneities in the Earth model are present. If sharp velocity gradients exist, the coefficients do not clearly decrease with increasing degree, but the group-velocity map tends to a more detailed one.

The algorithm used in solving expression (7) is also relevant for the degree of the expansion. By means of the singular value decomposition (S.V.D.) (Lanczos 1961), we solve the system of Eq. (7) in a proper way. Other possibilities are the total inversion algorithm (Tarantola and Valette 1982) or the Backus-Gilbert inversion (Backus and Gilbert 1967, 1968). Examples of the application of the total inversion algorithm are the papers of Angelier et al. (1982) and Lana and Correig (1987). With respect to the Backus-Gilbert inversion we can refer, for instance, to Nolet (1976) and Tanimoto and Anderson (1985). The linearity between

Table 1. Earthquake parameters. The numbers of the events correspond to those in Fig. 1. *CARL*, *MIR* and *MASC* identify, respectively, the regions of Carlsberg Ridge, Mid-Indian Rise and Mascarena Island Region

	Date	Latitude	Longitude	Origin time	Depth	Magnitude
1 CARL	04.0.572	5.200	62.100	0 h 27 m 34 s	58 km	5.1
2 MASC	06.19.76	−17.900	65.400	15 h 0 m 46 s	21 km	5.5
3 CARL	09.0.772	− 1.900	68.100	2 h 55 m 0 s	47 km	5.6
4 MIR	10.29.70	−40.900	80.500	2 h 23 m 25 s	33 km	5.5
5 MIR	11.22.76	−38.500	78.600	4 h 46 m 26 s	33 km	5.1
6 MASC	10.25.70	−13.700	66.300	12h 0 m 35 s	25 km	5.6
7 MIR	03.27.76	−38.900	78.100	8 h 49 m 32 s	35 km	5.2
8 MIR	02.19.77	−41.300	80.500	7 h 53 m 23 s	33 km	5.8
9 MIR	11.16.76	−41.800	80.100	18 h 20 m 49 s	18 km	5.3

the travel times and the coefficients, together with the simplicity and the speed of computation of the S.V.D. algorithm, make it advisable to use the S.V.D. algorithm in this case.

If all the eigenvalues, evaluated by the S.V.D. algorithm, are used in the solution of system (7), usually unrealistic Earth models appear. Such models are a consequence of including also the smallest eigenvalues. The existence of small eigenvalues is due to singularities in the system of equations. The existence of these singularities comes not only from the noise in the data, but also from the path coverage. It is obvious that there may be a certain number of paths which are very close to each other and that they generate very similar equations in (7). We must bear in mind that a certain degree of the expansion implies a minimum number of independent paths. Singularities are usually expected, and the crucial question here is the choice of a reasonable cut-off value l_0 which fixes the last eigenvalue that the algorithm will employ in the matrix inversion. Problems related to the proper choice of l_0 have been pointed out by Tanimoto and Anderson (1985), studying the upper mantle of the whole Earth, but without absolutely conclusive results about the proper cut-off value. When the group-velocity distribution is computed all over the Earth, the physical meaning of the evaluated coefficients is particularly relevant in deciding the cut-off value. In this case the coefficient A_{00} represents the inverse of the averaged group velocity (Nakanishi and Anderson, 1982). Following this interpretation, the fixed l_0 must involve a suitable value of A_{00} in agreement with some reasonable standard Earth model. The present application does not study the entire domain of the Earth's surface, and A_{00} has a different meaning. According to Eq. (4), if we integrate this expression over the whole Earth's surface, only the term with $n=0$ and $m=0$ contributes to the averaged slowness. In our case, integrating over part of the Earth's surface, the averaged slowness depends not only on the term with $n=0$, $m=0$ but also on higher terms which do not cancel now. We also think that the extension of the integration over the whole surface is meaningless, because our data are only related to a restricted domain of the Earth. The evaluation, in such a case, of both the cut-off value and the expansion degree must be done at the same time taking into consideration the following points:

A) The decreasing evolution of the travel-time residuals with an increasing degree and with different l_0.

B) To obtain coefficient values with a reasonable behaviour for the degree of the expansion.

C) Poor resolution in the kernels of the S.V.D. algorithm for most of the coefficients implies a superfluous degree, even though the residual has a good evolution. We must bear in mind that, according to Eq. (7), the kernel resolution matrix is defined by:

$$\boldsymbol{K}=\boldsymbol{M}^{-1}\boldsymbol{M}. \tag{12}$$

The matrix $\boldsymbol{K}$ is the identity matrix if $l_0=0$. On the other hand, $l_0>0$ leads to a matrix $\boldsymbol{K}$ which differs from the identity matrix. The coefficient which corresponds to the row of the $\boldsymbol{K}$ matrix that differs from the same row in the identity matrix has a poor resolution.

In short, the degree and the cut-off value l_0 arise as a result of the minimization of the travel-time residual, the correct evolution of the coefficients and the best kernel resolutions for most of them. With respect to the expansion degree, it is convenient to apply a window to the coefficients. By doing this we can remove or attenuate the ringing phenomena in the group-velocity maps. This phenomenon is very similar to that obtained when a short temporal signal is spectrally analysed. Because of the analogy between both situations we can use (Tanimoto and Anderson 1985) a classical Hamming window, substituting the length of the temporal signal by the number of the highest degree expansion used. If the slowness has sharp discontinuities, Gibbs phenomena (Kulhanek 1976) could appear when expression (4) is truncated. We assume that such discontinuities are not present in the slowness. Consequently, Gibbs phenomena will not appreciably affect the group-velocity maps.

The third and last point is the mathematical meaning of the cut-off operation. The generation of compatible solutions of linear or linearized systems of equations like (7), as a consequence of the smallest eigenvalues, is well established in Pous et al. (1985) and Lana and Correig (1986). The consequences and the physical meaning in our application will be discussed in the conclusions.

Application to the Indian Ocean

The theory and methodology developed above has been applied to a set of experimental group velocities of the fundamental mode of Rayleigh waves, evaluated for the Indian Ocean. These group velocities are obtained, after standard instrumental correction of the records (Chandra, 1970), by standard spectral analysis of the vertical component of the seismic records (Herrmann 1973, 1978). These records correspond to several WWSSN stations surrounding the Indian Ocean and to earthquakes with magnitudes between 5 and

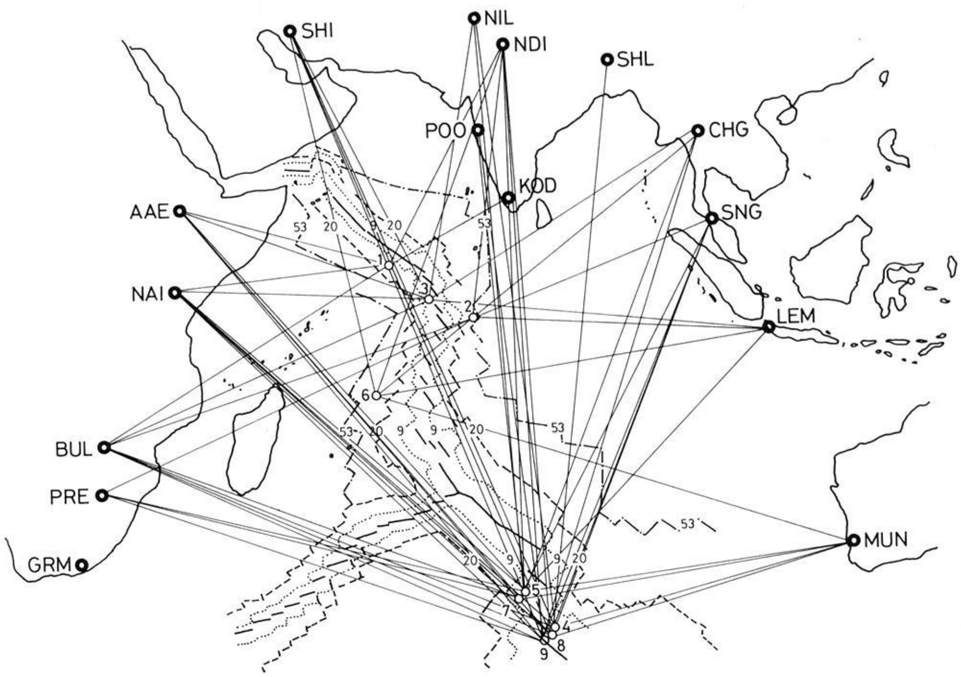

Fig. 1. Path coverage for the Indian Ocean. The *codes* correspond to the WWSSN stations used. The *numbers* correspond to the nine events from which seismic records were obtained. A scheme of ridges with the Rodrigues triple junction and the distribution of lithospheric ages in units of million years are also included

Table 2. Set of coefficients obtained at 15, 30, 40, 50 and 60 s, fourth-degree expansion and a cut-off value of 0.05

	15 s	30 s	40 s	50 s	60 s
A_{00}	0.379 E+00	0.214 E+00	0.219 E+00	0.233 E+00	0.207 E+00
A_{10}	−0.106 E+00	−0.651 E−01	−0.428 E−01	−0.883 E−01	−0.728 E−01
A_{11}	0.172 E+00	0.956 E−01	0.125 E+00	0.897 E−01	0.877 E−01
A_{20}	0.184 E+00	−0.675 E−01	−0.948 E−01	−0.390 E−01	−0.729 E−01
A_{21}	−0.294 E+00	−0.180 E−02	−0.448 E−01	0.757 E−01	−0.135 E−01
A_{22}	−0.222 E+00	−0.134 E+00	−0.102 E+00	−0.114 E+00	−0.135 E+00
A_{30}	−0.105 E+00	0.369 E−02	0.136 E−02	0.101 E−03	0.105 E−01
A_{31}	0.185 E+00	−0.165 E−01	−0.198 E−01	−0.397 E−01	−0.254 E−01
A_{32}	−0.265 E+00	0.210 E−01	−0.264 E−01	0.505 E−01	0.113 E−01
A_{33}	−0.213 E−01	−0.371 E−01	−0.162 E−01	−0.519 E−01	−0.389 E−01
A_{40}	0.134 E+00	−0.445 E−01	−0.239 E+00	−0.511 E−01	−0.710 E−01
A_{41}	0.531 E−02	0.204 E+00	0.147 E+00	0.606 E−01	0.683 E−01
A_{42}	−0.130 E−01	0.348 E−01	0.102 E+00	0.889 E−01	0.967 E−02
A_{43}	−0.122 E+00	−0.864 E−01	−0.368 E−01	−0.773 E−02	−0.613 E−01
A_{44}	−0.908 E−01	−0.356 E−01	0.146 E−01	0.144 E−01	−0.136 E−01
B_{11}	0.381 E+00	0.265 E+00	0.260 E+00	0.274 E+00	0.260 E+00
B_{21}	0.710 E−01	−0.780 E−01	−0.317 E−01	−0.116 E+00	−0.856 E−01
B_{22}	0.130 E+00	0.117 E+00	0.129 E+00	0.123 E+00	0.108 E+00
B_{31}	0.268 E+00	0.100 E−01	−0.790 E−02	0.479 E−01	0.491 E−02
B_{32}	−0.177 E+00	0.117 E−01	−0.244 E−01	0.900 E−01	0.221 E−02
B_{33}	−0.141 E+00	−0.189 E−01	−0.932 E−02	0.144 E−01	−0.242 E−01
B_{41}	0.512 E−01	−0.143 E+00	−0.156 E+00	−0.854 E−01	−0.117 E+00
B_{42}	−0.242 E+00	0.437 E−01	−0.848 E−01	0.252 E−01	−0.189 E−01
B_{43}	0.219 E+00	0.422 E−01	0.988 E−01	−0.766 E−01	−0.241 E−01
B_{44}	0.147 E+00	0.861 E−01	0.112 E+00	0.783 E−01	0.710 E−01

6. The events used, and their main characteristics, are listed in Table 1. Source group delay has been neglected. The distribution of the paths in the Indian Ocean and the main surface tectonic features are shown in Fig. 1.

Following the methodology discussed above, a suitable expansion degree and a suitable cut-off value of 0.05 for the S.V.D. algorithm have been fixed. The Euclidian norms of the travel-time residuals divided by the number of paths, at a period of 15 s for the first four degrees, for instance, are: 110.6, 101.0, 89.2, and 58.9, given in units of s^2. These residuals, computed without cut-off value, are only slightly different from those calculated with a cut-off value. These residuals imply an averaged difference of 9 s between the experimental travel times and the theoretical ones evaluated from expression (5) with the coefficients obtained solving system (7). This averaged difference of 9 s results in an upper limit of uncertainty in the third decimal place of the group velocities according to Eq. (11). This assessment is a conse-

Table 3. Set of coefficients obtained at 15, 30, 40, 50 and 60 s, third-degree expansion and a cut-off value of 0.05

	15 s	30 s	40 s	50 s	60 s
A_{00}	0.326E+00	0.283E+00	0.275E+00	0.280E+00	0.280E+00
A_{10}	−0.111E+00	−0.977E−01	−0.101E+00	−0.191E+00	−0.152E+00
A_{11}	0.288E+00	0.133E+00	0.224E+00	0.735E−01	0.106E+00
A_{20}	−0.912E−01	−0.711E−01	−0.685E−01	−0.307E−01	−0.441E−01
A_{21}	−0.863E−01	−0.301E−01	−0.695E−01	−0.347E−01	−0.336E−01
A_{22}	−0.600E−01	−0.110E+00	−0.624E−01	−0.106E+00	−0.111E+00
A_{30}	−0.190E+00	−0.559E−01	−0.126E+00	−0.109E+00	−0.978E−01
A_{31}	−0.131E+00	0.541E−02	−0.881E−01	0.802E−02	−0.787E−01
A_{32}	−0.348E−02	−0.624E−01	−0.364E−01	−0.133E+00	−0.126E+00
A_{33}	0.231E+00	0.983E−01	0.162E+00	0.231E−01	0.607E−01
B_{11}	0.339E+00	0.325E+00	0.290E+00	0.313E+00	0.315E+00
B_{21}	−0.719E−01	−0.767E−01	−0.671E−01	−0.156E+00	−0.118E+00
B_{22}	0.233E+00	0.110E+00	0.183E+00	0.586E−01	0.909E−01
B_{31}	0.132E+00	0.679E−01	0.115E+00	0.871E−02	0.735E−01
B_{32}	0.542E−01	0.729E−01	0.588E−01	0.817E−01	0.554E−01
B_{33}	−0.906E−01	0.435E−01	−0.706E−01	0.545E−01	0.157E−01

Table 4. Graphical representation of the kernel resolution matrix at a period of 15 s, an expansion of fourth degree and a cut-off value of 0.05. The elements of the symmetric matrix have been reduced to values ranging from 0 to 10, which are proportional to their absolute values between 0 and 1. The rows are associated, from the top to the bottom of the table, with the coefficients A_{00}, A_{10}, ... B_{43}, B_{44}

3																								
1	2																							
1	0	2																						
0	1	0	3																					
0	1	1	0	4																				
1	0	1	1	0	4																			
0	1	0	1	1	0	3																		
0	0	0	1	1	0	0	3																	
0	1	0	0	2	0	1	1	4																
0	0	1	0	0	0	0	0	0	3															
0	0	0	1	0	0	1	0	0	0	9														
0	0	0	0	0	0	1	1	0	0	0	9													
1	1	0	0	0	1	0	1	1	1	0	0	9												
0	0	0	0	1	0	1	0	1	0	0	0	0	9											
0	0	1	0	0	1	0	1	0	0	0	0	0	0	9										
3	1	1	1	0	3	0	0	1	0	0	0	0	0	0	4									
0	3	0	0	0	0	2	0	3	0	0	0	0	0	0	0	5								
1	0	3	1	0	1	0	1	0	2	0	0	0	0	1	1	0	4							
1	1	0	4	0	1	1	1	1	0	1	0	1	0	0	0	1	0	6						
0	1	1	0	4	0	1	1	1	0	0	0	1	2	0	1	1	0	1	5					
0	0	1	0	1	3	0	1	0	0	0	0	0	0	2	1	0	2	0	1	4				
0	1	0	0	0	0	3	0	0	0	0	0	0	0	0	0	1	0	0	0	0	9			
0	0	0	0	1	0	0	2	1	0	0	0	0	0	0	0	0	1	0	0	0	0	9		
0	0	1	0	0	0	1	1	2	0	0	0	0	0	0	0	1	0	0	0	1	0	0	9	
1	0	1	1	0	1	0	0	0	3	0	0	1	0	0	1	0	0	0	0	1	0	0	0	8

Table 5. Set of coefficients for a third- and fourth-degree expansion at a period of 15 s. No cut-off value has been used. These coefficients are very different from those in Tables 2 and 3

A_{00}	−0.347E+02	0.715E+04
A_{10}	−0.545E+01	0.196E+04
A_{11}	0.140D+02	−0.217E+04
A_{20}	0.112E+02	−0.214E+04
A_{21}	0.430E+00	−0.561E+03
A_{22}	0.852E+01	−0.355E+04
A_{30}	0.932E+00	−0.537E+03
A_{31}	−0.139E+01	0.181E+03
A_{32}	0.797E+00	−0.574E+03
A_{33}	−0.122E+01	0.835E+03
A_{40}		0.452E+02
A_{41}		0.327E+02
A_{42}		0.736E+02
A_{43}		0.756E+02
A_{44}		0.785E+02
B_{11}	0.346E+02	−0.801E+04
B_{21}	0.441E+01	−0.188E+04
B_{22}	−0.872E+01	0.207E+04
B_{31}	−0.257E+01	0.714E+03
B_{32}	−0.809E−01	0.374E+03
B_{33}	−0.351E+00	0.838E+03
B_{41}		0.112E+03
B_{42}		−0.381E+02
B_{43}		0.654E+02
B_{44}		−0.132E+03

quence of the standard deviations computed by means of Eqs. (8)–(10). As we can see, there is a significant decrease in the residuals from the first to the fourth degree.

It can be seen that the errors in travel times are very similar to the travel-time residuals of the fourth-degree expansion, by comparing pairs of travel times for similar trajectories. Consequently, neglecting the anisotropy effect and remembering the linear character of the problem, we can assume that data residuals are of the same magnitude as data errors. We can also compare the Euclidian norm of the residual with the Euclidian norm of the differences between the experimental travel times and those computed for a spherical symmetric Earth such as the PREM: model (Dziewonski and Anderson 1981). In such a way, a variance reduction between 35% and 45% is obtained.

Tables 2 and 3 show the set of coefficients obtained for degrees 4 and 3, respectively, for all periods as well as the common value of l_0 that leads system (7) to the proper solution. As Nakanishi and Anderson (1982) show, coefficients belonging to higher degrees are usually small corrections of those calculated for smaller degrees, if great lateral heterogeneities are missing in the medium. Tables 2 and 3 illustrate this behaviour, where some of the higher-degree coefficients are also slightly smaller than the lower ones. This situation could not only be the result of an insufficient

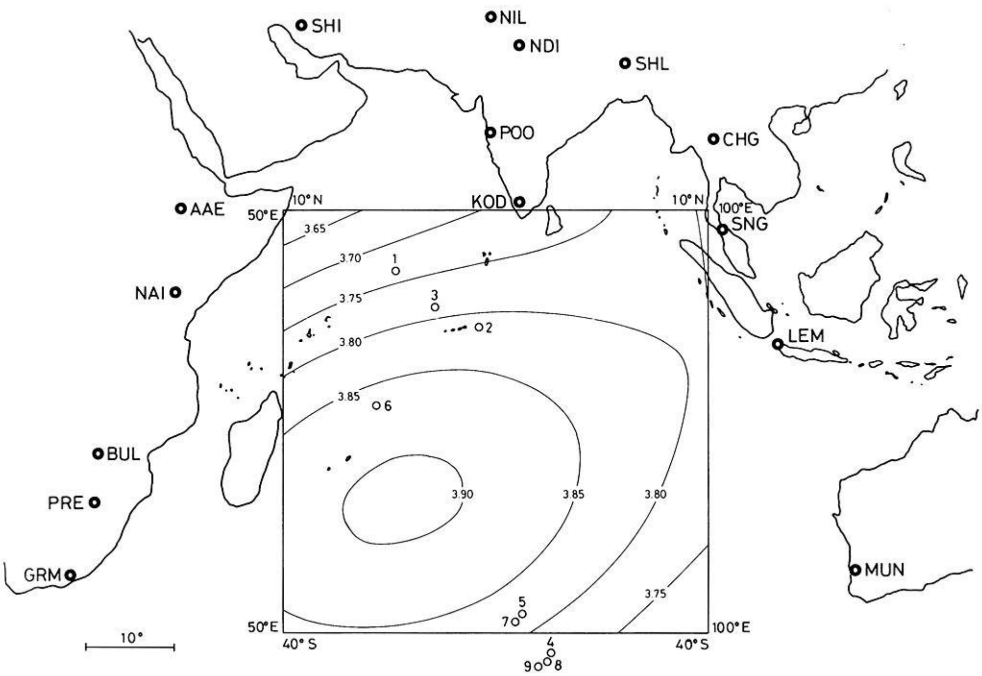

Fig. 2. Group-velocity map for a period of 30 s and a second-degree expansion. Isolines are given in units of km/s. The *numbers* correspond to the events of Table 1

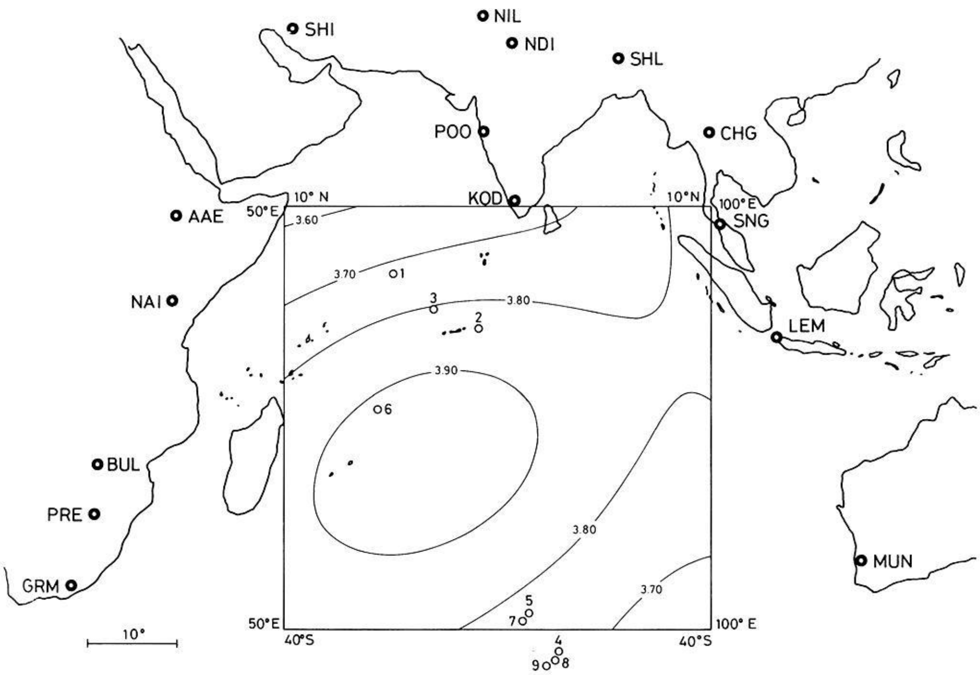

Fig. 3. Same as Fig. 2, with a third-degree expansion

degree of the expansion, but also due to sharp group-velocity gradients. A higher degree could be attempted, giving smaller travel-time residuals. Table 4 shows the resolution kernel for a fourth-degree expansion at 15 s. It can be seen that coefficients A_{4m}, B_{4m}, $(m=1, \ldots, 4)$ have a very good resolution, whereas some of the rest have a very poor one. Through the inversion process, a decrease of the kernel quality, when the expansion degree increases has been observed. Consequently, very poor resolution for all of the coefficients would be found in expansions with a degree greater than four. The kernel evolution is, of course, a direct consequence of the singularities and cut-off values. Taking into account the restrictions discussed in the methodology, an expansion of fourth degree and a cut-off value of 0.05 looks reasonable for all periods. Third- and fourth-degree kernels are very similar. Though a third-degree expansion would be acceptable, its travel-time fit is worse than that associated with the fourth degree. In addition, the fourth degree gives more detailed group-velocity maps. We can obtain very good kernels' with second-degree expansions, but the corresponding group-velocity maps give an extremely simplified view of the medium.

It is important to point out that if a cut-off value smaller than l_0 is used, the coefficients of the expansion lose all their; physical meaning. Table 5 shows the wrong coefficients obtained for third and fourth degrees at a period

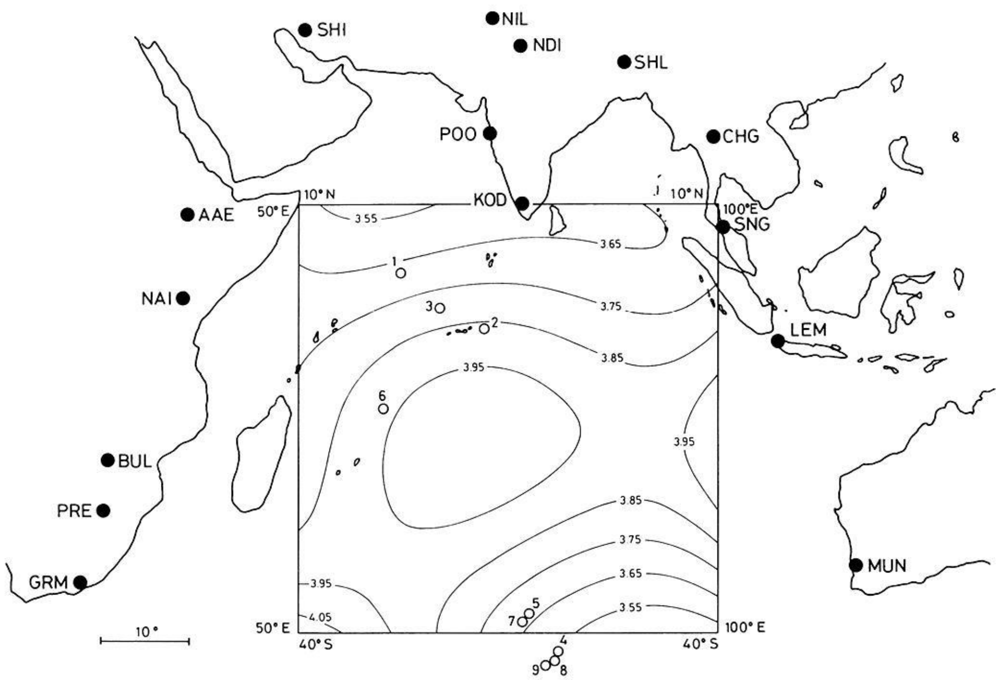

Fig. 4. Same as Fig. 2, with a fourth-degree expansion

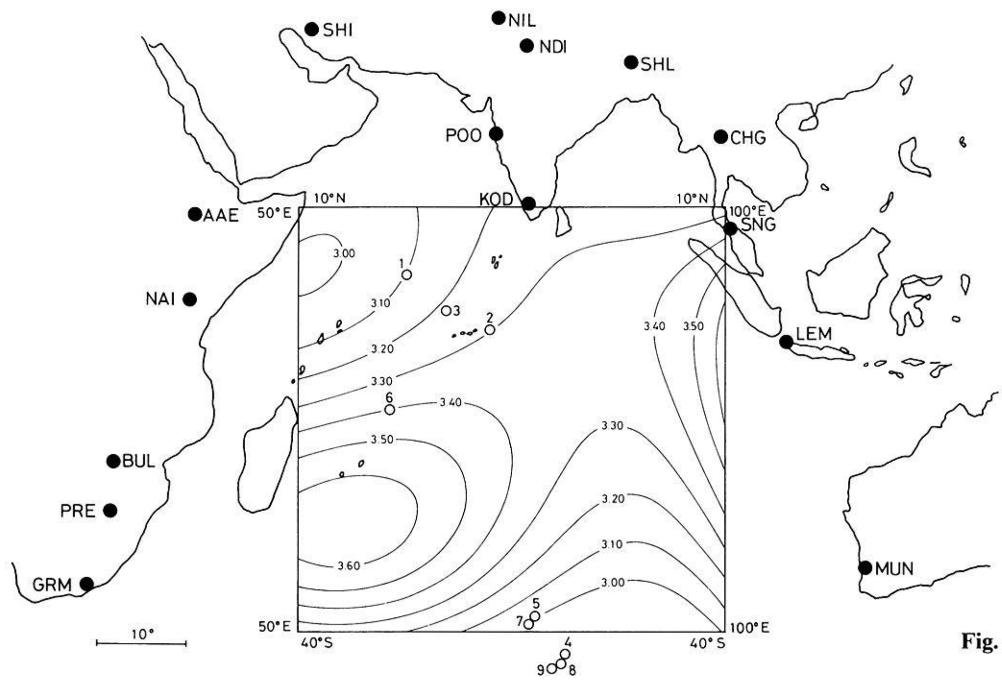

Fig. 5. Same as Fig. 2, for a period of 15 s

of 15 s; no cut-off values has been used. Notice the unreasonable jump in the coefficient values when changing from one degree to the other. In a similar way, the unacceptable values of the coefficients in Table 5 become evident, if they are compared with those in Tables 2 and 3.

Figures 2 and 3, together with Fig. 4, show the group-velocity evolution through an increasing degree of expansion at a period of 30 s. Figures 2 and 3 correspond to expansion of second and third degree, respectively, and have been computed according to the methodology discussed, with a suitable cut-off value for each degree slightly different from 0.05. From the set of maps at 30 s one can deduce that very similar features are developed by third and fourth degrees. The second degree with a suitable l_0 expansion generates the same robust features as the greater-degree maps do, but in a more simplified and poorly detailed way.

Figures 4–8 are group-velocity distributions for the Indian Ocean at periods of 30, 15, 40, 50 and 60s. All of them correspond to fourth-degree expansions. There is a small evolution through the five maps where the robust common features are a maximum group velocity near the Rodrigues triple junction, another maximum just south of the Indonesian Arc, one saddle point at both sides of the central maximum and a minimum just on the Indian Coast.

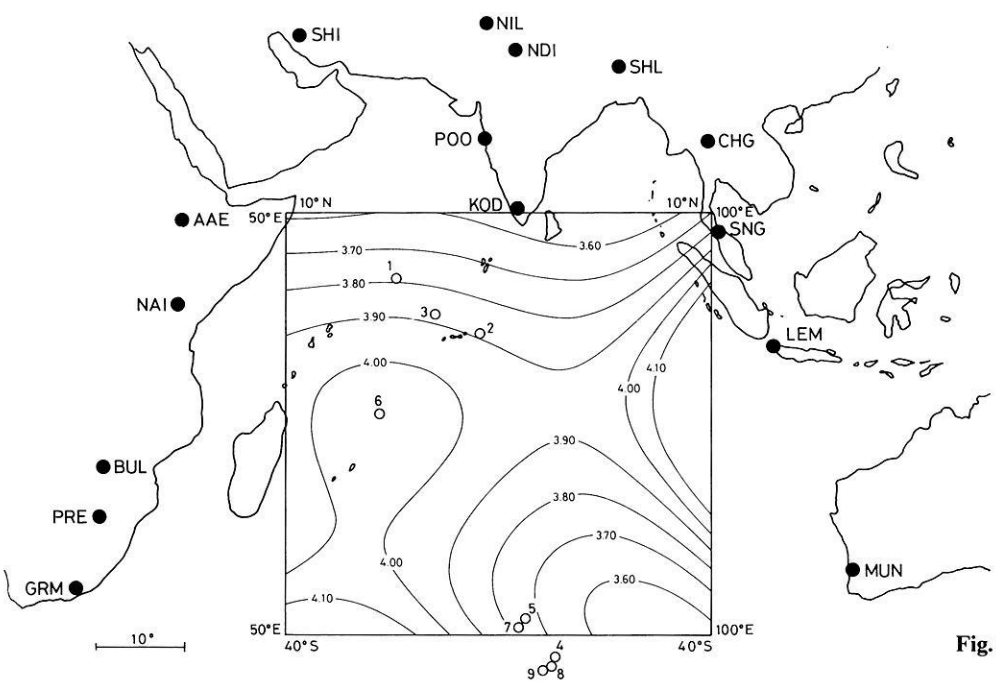

Fig. 6. Same as Fig. 2, for a period of 40 s

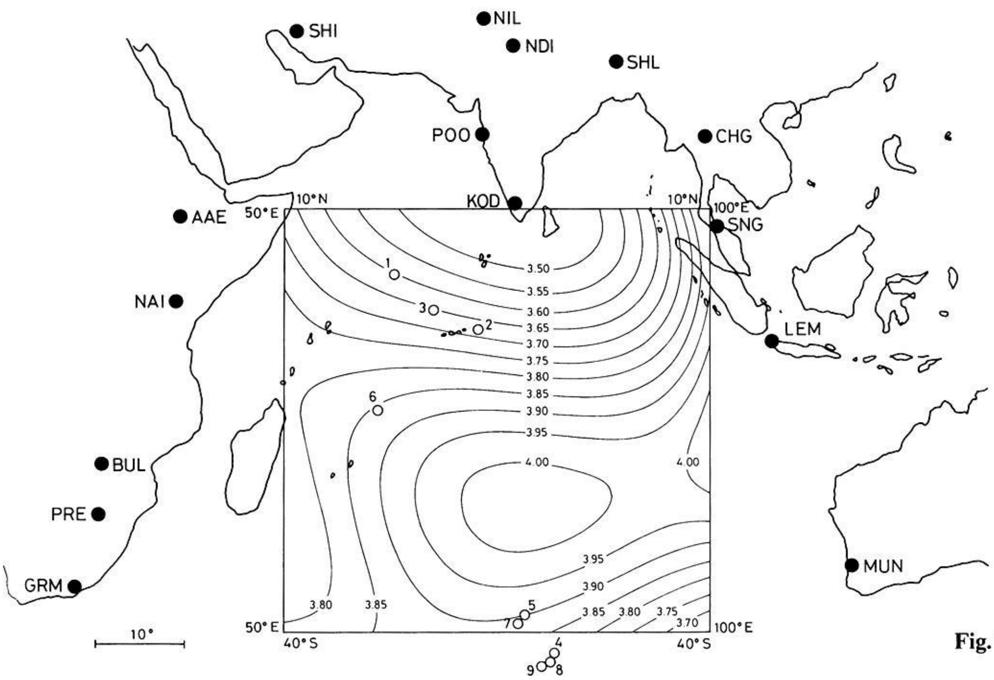

Fig. 7. Same as Fig. 2, for a period of 50 s

Conclusions

Using a set of group velocities computed by a standard spectral analysis program, a methodology for surface harmonic expansions in restricted regions of the Earth's surface is developed. By means of this methodology one can establish the cut-off value for the S.V.D. algorithm and the degree of the expansion. Both the expansion degree and the cut-off value are determined from three conditions:

1) First, the determination of the smallest travel-time residual

2) Second, the search for expansion coefficients with physical meaning

3) Third, the retrieval of good resolution of the kernel for a significant number of coefficients

It is relevant to point out that the combination of these points systematizes two aspects of the paper of Nishimura and Forsyth (1985); namely, a better treatment of the singularities and an efficient system to define the proper degree of the spherical harmonic expansion. This last aspect is very important due to the fact that the easy process of studying only the minimization of the travel-time residuals (Nakanishi and Anderson 1982) does not always define the proper degree.

The cut-off operation means that other compatible solutions can be reached. This assertion has been discussed and

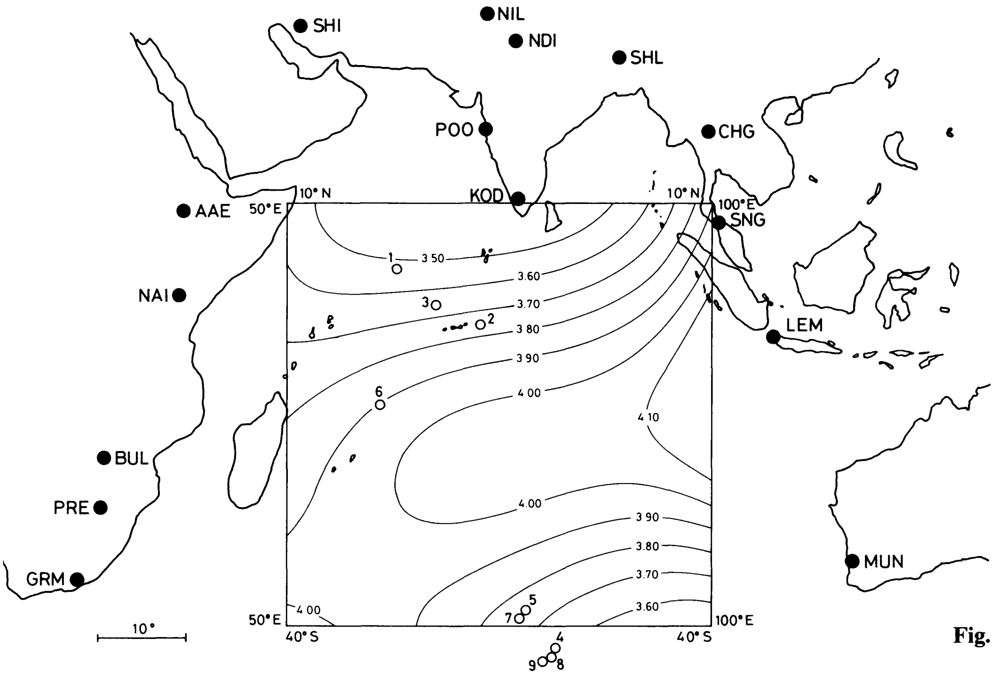

Fig. 8. Same as Fig. 2, for a period of 60 s

exercised in other aspects of seismology by Pous et al. (1985) and Lana and Correig (1986).

Coming to the specific results for the Indian Ocean, it is important to point out the existence of the same robust features in all velocity distribution maps. These robust features are present in both sequences of maps shown here: one for increasing expansion degree at a given period; the other for different periods and a given expansion degree. Perhaps the most relevant feature are the high velocities near the triple junction.

Comparing the map at 30-s period with the world-wide distribution of group velocity at the same period obtained by Sato and Santo (1969), we find that the relevant maximum is located at the same place, but that our map is more detailed because of better coverage over a smaller domain. We obtain even greater similarity when a smaller expansion degree is used, but then we lose details.

The map shown at 60 s can be approximately compared with that of Montagner (1986) at 75 s. The similarities seen, as in the case before, are the robust features. The minimum in the southeast corner of the map has its correspondence in Montagner's map. The maximum value of our group-velocity distribution just south of the islands of Sumatra and Java also has its correspondence in Montagner's map, and the south part of our map is also in agreement. Another minimum can be assumed in our map south of the Arabian peninsula, which is also well define in Montagner's paper. A different distribution of group velocities appears near the Indian peninsula. We think this effect is due to the poor coverage we had for this region (Fig. 1) and perhaps also due to the effect of the continental crust, corrected in Montagner (1986). From this last point we may conclude that coverage is important. Another point that reinforces this conclusion is the above discussion for the period 30 s; when the second-degree expansion fits Sato and Santo's maps, but a fourth-degree expansion develops a more accurate description.

The evolution of all the common robust features, observed through the maps as we increase the period, indicates good correlation between the shallow and intermediate structure with surface tectonics down to a depth of 60 km. This result is reinforced by a similar correlation for deeper structures pointed out by Montagner (1986), if we bear in mind the agreement between his map at 75 s and our map at 60 s.

Group-velocity dispersion curves can, in fact, be inferred from these expansions by increasing the number of periods; one then obtains slightly different dispersion curves for different age regions of the Indian Ocean lithosphere. Partial derivatives of group velocities (Rodi et al., 1975) can be used to retrieve the shallow and intermediate lithosphere structure (depth range 10–70 km) missed by Montagner (1986), because of the very long period he used. In this way it will be possible to compare computed models of the lithosphere with the location of ridges and distribution of lithospheric ages. As a first step, the map at 15 s shows good correlation between 10- to 53-million-year lithosphere and low group velocities. Regions with lithospheric age greater than 53 million year have higher group velocities. In short, the present paper establishes rough lines for a study which may confirm Montagner's lithospheric models at intermediate periods.

Acknowledgements. This work has been supported by the C.I.R.I.T. from "Govern de la Generalitat de Catalunya" (Spain). We also want to thank the members of the "Institut de Physique du Globe de Paris" (France), especially Dr R. Madariaga and Dr. A. Deschamps, for facilities supplied in the digitization of the WWSSN seismic records used. J.J. Egozcue (E.T.S.E.C.C.P.), Universidad Politècnica de Barcelona, made helpful comments.

References

Angelier, J., Tarantola, A., Valettte, B., Manoussis, S.: Inversion of field data in fault tectonics to obtain the regional stresses. (I). Single phase populations: a new method of computing the stress tensor. Geophys. J. R. Astron. Soc. **69**, 607–621, 1982

Backus, G.E., Gilbert, J.F.: Numerical application of a formalism for geophysical inverse problems. Geophys. J. R. Astron. Soc. **13**, 247–276, 1967

Backus, G.E., Gilbert, J.F.: The resolving power of gross Earth data. Geophys. J. R. Astron. Soc. **16**, 169–205, 1968

Chandra, U.: Analysis of body waves spectra for earthquake energy determination. Bull. Seismol. Soc. Am. **60**, 539–563, 1970

Coode, A.M.: The spherical harmonic analysis of major tectonic features. In: Mantles of the Earth and terrestrial planets, Runcorn, S.K., ed. New York: Interscience publishers 1967

Courant, R., Hilbert, D.: Methods of mathematical physics. New York: Interscience publishers 1962

Dziewonski, A.M.: Mapping the lower mantle: determination of lateral heterogeneity in P velocity up to degree and order 6. J. Geophys. Res. **89**, 5929–5952, 1984

Dziewonski, A.M., Anderson, D.L.: Preliminary reference Earth model. Phys. Earth Planet. Inter. **25**, 297–356, 1981

Ellsasser, H.W.: Expansion of the hemispheric meteorological data in anti-symmetric surface spherical harmonics. J. Appl. Meteorol. **5**, 263–276, 1966

Herrmann, R.B.: Some aspects of band-pass filtering of surface waves. Bull. Seismol. Soc. Am. **63**, 663–671, 1973

Herrmann, R.B.: Computer programs in earthquakes seismology. Surface wave programs. Hermann, R.B., ed. Saint Louis University, 1978

Horai, K., Simmons, G.: Spherical harmonic analysis of the terrestrial heat flow. Earth Planet. Sci. Lett. **6**, 386–394, 1969

Kaula, W.M.: Statistical and harmonic analysis of gravity. J. Geophys. Res. **64**, 2401–2421, 1959

Kulhanek, O.: Introduction to digital filtering in geophysics. Developments in solid Earth geophysics, vol 8, 168 pp. New York: Elsevier 1976

Lana, X., Correig, A.M.: The retrieval of the seismic moment tensor from first order perturbation theory and computation of compatible models. J. Geophys. **60**, 167–174, 1986

Lana, X., Correig, A.M.: An example of stress tensor distribution deduced from the aftershocks of the November 23, 1980 southern Italy earthquake. Tectonophysics 1987 (in press)

Lanczos, C.: Linear differential operators. London: Van Nostrand Company 1961

Mitchell, B.J., Yu, G.K.: Surface waves dispersion regionalized velocity models, and isotropy of the Pacific crust and upper mantle. Geophys. J. R. Astron. Soc. **63**, 497–514, 1980

Montagner, J.P.: 3-D dimensional structure of the Indian Ocean inferred from long period surface waves. Geophys. Res. Lett. **13**, 315–318, 1986

Nakanishi, I., Anderson, D.L.: Worldwide distribution of group velocity of mantle Rayleigh waves as determined by spherical harmonic inversion. Bull. Seismol. Soc. Am. **72**, 1185–1194, 1982

Nataf, H.C., Nakanishi, I., Anderson, D.L.: Anisotropy and shear velocity heterogeneities in the upper mantle. Geophys. Res. Lett. **11**, 109–112, 1984

Nishimura, C.E., Forsyth, D.W.: Anomalous Love waves phase velocities in The Pacific: sequential pure-path and spherical harmonic inversion. Geophys. J. R. Astron. Soc. **81**, 389–407, 1985

Nolet, G.: Higher modes and the determination of upper mantle structure. Doctoral Thesis, University of Utrecht, 1976

Pous, J., Lana, X., Correig, A.M.: Generation of Earth stratified models compatible with both ellipticity and phase velocity observations of Rayleigh waves. Pure Appl. Geophys. **123**, 870–881, 1985

Rodi, W.L., Glover, P., Li, T.M.C., Alexander, S.S.: A fast, accurate method for computing group-velocity partial derivatives for Rayleigh and Love waves. Bull. Seismol. Soc. Am. **65**, 1105–1114, 1975

Sato, Y., Santo, T.: World wide distribution of the group velocity of Rayleigh waves as determined by dispersion data. Bull. Earthq. Res. Inst. **47**, 31–41, 1969

Tanimoto, T., Anderson, D.L.: Lateral heterogeneity and azimuthal anisotropy of the upper mantle: Love and Rayleigh waves 100–250 s. J. Geophys. Res. **96**, 1842–1858, 1985

Tarantola, A., Valette, B.: Generalized non linear inverse problem solved by using the least square criterion. Rev. Geophys. Space Phys. **20**, 219–232, 1982

Woodhouse, J.H., Dziewonski, A.M.: Mapping the upper mantle: three dimensional modeling of Earth structure by inversion of seismic waveforms. J. Geophys. Res. **89**, 5953–5986, 1984

Yu, G.K., Mitchell, B.J.: Regionalized shear velocity models of the Pacific upper mantle from observed Love and Rayleigh waves dispersion. Geophys. J. R. Astron. Soc. **57**, 311–341, 1979

Received November 7, 1986; revised version May 29, 1987
Accepted June 22, 1987